Published in final edited form as:
Matrix Biol. 2014 July ; 37: 35–48. doi:10.1016/j.matbio.2014.02.003.

Control of Organization and Function of Muscle and Tendon by Thrombospondin-4

Ella G. Frolova[1], **Judith Drazba**[3], **Irene Krukovets**[1], **Volodymyr Kostenko**[2], **Lauren Blech**[1], **Christy Harry**[1], **Amit Vasanji**[4], **Carla Drumm**[1], **Pavel Sul**[1], **Guido J. Jenniskens**[5], **Edward F. Plow**[1], and **Olga Stenina-Adognravi**[1,*]

[1]Department of Molecular Cardiology, Lerner Research Institute, Cleveland Clinic, Cleveland, OH 44195 [2]Department of Neurology, Neuromuscular Section, Lerner Research Institute, Cleveland Clinic, Cleveland, OH 44195 [3]Imaging Core, Lerner Research Institute, Cleveland Clinic, Cleveland, OH 44195 [4]Biomedical Imaging and Analysis Core, Lerner Research Institute, Cleveland Clinic, Cleveland, OH 44195 [5]Department of Biochemistry 194, University Medical Center, NCMLS and ModiQuest Research BV, Nijmegen, The Netherlands

Abstract

Thrombospondins (TSP) are multifunctional proteins that are deposited in the extracellular matrix where they directly affect the function of vascular and other cell types. TSP-4, one of the 5 TSP family members, is expressed abundantly in tendon and muscle. We have examined the effect of TSP-4 deficiency on tendon collagen and skeletal muscle morphology and function. In *Thbs4*$^{-/-}$ mice, tendon collagen fibrils are significantly larger than in wild-type mice, and there is no compensatory over-expression of TSP-3 and TSP-5, the two TSPs most highly homologous to TSP-4, in the deficient mice. TSP-4 is expressed in skeletal muscle, and higher levels of TSP-4 protein are associated with the microvasculature of red skeletal muscle with high oxidative metabolism. Lack of TSP-4 in *Medial soleus*, red skeletal muscle with predominant oxidative metabolism, is associated with decreased levels of several specific glycosaminoglycan modifications, decreased expression of a TGFβ receptor beta-glycan, decreased activity of lipoprotein lipase, which associates with vascular cell surfaces by binding to glycosaminoglycans, and decreased uptake of VLDL. The soleus muscle is smaller and hind- and fore-limb grip strength is reduced in *Thbs4*$^{-/-}$ mice compared to wild-type mice. These observations suggest that TSP-4 regulates the composition of the ECM at major sites of its deposition, tendon and muscle, and the absence of TSP-4 alters the organization, composition and physiological functions of these tissues.

*Corresponding author address: Olga Stenina-Adognravi, Department of Molecular Cardiology, Lerner Research Institute, Cleveland Clinic, 9500 Euclid Avenue/NB50, Cleveland, OH 44195; stenino@ccf.org, Phone: 216-444-9057, Fax: 216-445-8204.

Keywords

thrombospondin-4; skeletal muscle; tendon; glycosaminoglycans

1. INTRODUCTION

Thrombospondins (TSPs) are matricellular glycoproteins (Adams, 2001; Adams and Lawler, 2004; Bornstein, 1995, 2001; Mosher and Adams, 2012; Murphy-Ullrich and Iozzo, 2012). TSPs have not been shown to provide structure to the extracellular matrix (ECM), as do the collagens or elastins, but they are known to regulate many of the protein-protein and protein-cell interactions within the ECM (Adams, 2001; Bornstein, 2001). The functions of the TSPs depend upon their interactions with other ECM constituents, i.e., other proteins, proteoglycans, glycosaminoglycans (GAGs) and cell-surface receptors, including multiple integrins, CD36 and CD47 (IAP) (Adams, 2001; Chen et al., 2000; Stenina et al., 2007). These interactions allow the TSPs to influence diverse cellular responses, such as attachment, spreading, motility, proliferation, apoptosis, and responses to proteases, growth factors and cytokines (Adams, 2001). TSPs are synthesized by many different cell types, and their expression is often regulated, allowing them to exert control over many different cellular responses (Adams and Lawler, 2004; Roberts et al., 2012; Sweetwyne and Murphy-Ullrich, 2012). The five TSP family members are each encoded by a different gene. They all carry a common signature, a highly homologous C-terminal part that includes calcium-binding (type 3) repeats and EGF-like domains (type 2 repeats) (Misenheimer and Mosher, 2005). The N-terminal part of each TSP is distinct (Adams, 2001; Chen et al., 2000). Based on their domain structure and oligomerization status, the TSPs can be divided into two groups: members of subgroup A (TSP-1, TSP-2) form trimers, and members of subgroup B (TSP-3, TSP-4, TSP-5) form pentamers (Engel, 2004). Despite the high degree of homology among the TSP family members, the promoters of the TSP genes, the regulatory regions of their mRNAs and, as a result, their tissue expression patterns are quite distinct, suggesting that each TSP may have unique functions.

Thrombospondin-4 (TSP-4), a member of subgroup B, was first described in 1993 by Lawler et al based on detection of its mRNA in *Xenopus laevis* (Lawler et al., 1993). Subsequent studies have indicated that TSP-4 mRNA is expressed at high levels in tendon and muscle as well as in neural and osteogenic tissues (Arber and Caroni, 1995; Hauser et al., 1995). TSP-4 protein has also been detected in brain capillaries (Stenina et al., 2003). Recent interest in TSP-4 has been stimulated by the demonstration that the human gene (*THBS4*) encoding for TSP-4 contains a single nucleotide polymorphism, which is expressed at high frequency in Caucasians and is associated with a significantly increased risk of premature myocardial infarction (Cui et al., 2006; Cui et al., 2004; Kato T, 2003; McCarthy et al., 2004; Stenina et al., 2004; Topol et al., 2001; Walton B, 2003; Wessel et al., 2004; Yamada et al., 2002).

Mice with inactivated genes for TSP-1, TSP-2, TSP-3 and TSP-5 (also known as cartilage oligomeric matrix protein or COMP) have been described (Hankenson et al., 2005; Kyriakides et al., 1998; Lawler et al., 1998; Svensson et al., 2002). Inactivation of these individual genes is not embryonically lethal, and the spontaneous phenotype of the adult

mice is largely unremarkable. However, when each of the TSP knock-out (KO) mice is challenged, specific abnormal responses have been noted. We recently reported that TSP-4 regulates local vascular inflammation, and the lack of TSP-4 delays the development of atherosclerotic lesions in a mouse model and results in fewer inflammatory lesion (Frolova et al., 2010). We and others reported that in myocardium, TSP-4 regulates ECM production, and the deficiency in TSP-4 causes increased fibrosis in response to pressure overload and negatively affects the cardiomyocytes function (Cingolani et al., 2011; Frolova et al., 2012; Lynch et al., 2012). TSP-4 controls important physiological and pathological processes in nervous system (Risher and Eroglu, 2012).

In the present study, we have focused on the distribution and function of TSP-4 in two major tissues of its deposition, tendon and muscle, and have examined the effects of its deficiency on the tendon and muscle structure and function. These tissues represent ~40% of human body weight, are a rich source of TSP-4 in humans (Arber and Caroni, 1995; Lawler et al., 1993), and deficiencies of TSPs have significant functional consequences in muscle and tendon (Adams and Lawler, 1994; Gilsohn and Volk; Kyriakides et al., 1998). Our results suggest that TSP-4 is critically required for the maintenance of ECM composition, structure and function at the cellular level and at the level of the whole limb.

2. RESULTS

2.1. *Thbs4*$^{-/-}$ mice

The TSP-4 deficient mice appeared normal at birth and displayed no obvious phenotype during their early and adult development. Their lifespan was similar to that of WT mice. There was a slight decrease (10–15%) in body weight of the *Thbs4*$^{-/-}$ mice with age although the mice appeared to be healthy. The skeletal systems of the *Thbs4*$^{-/-}$ and WT control mice were imaged using a custom-built micro-computed tomography system (Cleveland Clinic, Cleveland, OH) at 30μm voxel resolution and visualized using the VolSuite 3D rendering software (Ohio SuperComputer Center, Columbus, OH). The resulting data suggested that the abnormality in bone density and structure observed in the *Thbs3*$^{-/-}$ mice (Hankenson et al., 2005) was not present in the *Thbs4*$^{-/-}$ mice. Furthermore, skeletal anatomic aberrations were absent by visual inspection. In this work, we focused our analyses on the two tissues, tendon and muscle, in which abundant TSP-4 expression had been reported (Arber and Caroni, 1995; Hauser et al., 1995).

2.2. TSP-4 expression in tendon

TSP-4 shares up to 82% homology with TSP-3 and TSP-5 in the highly conserved carboxy-terminal region (Adams, 2004). We previously reported that the levels of other TSP-3 and TSP-5 were not changed in the blood vessel wall of *Thbs4*$^{-/-}$ mice (Frolova et al., 2010). We examined the expression patterns of TSP-3 and TSP-5 in tendon and skeletal muscle of WT and *Thbs4*$^{-/-}$ mice and found that their expression is not changed, and there is no compensation for the deficiency in TSP-4. In tendons of the WT triceps muscle, TSP-4 and TSP-3 are expressed in a non-overlapping fashion intersecting each other at an angle in WT mice (Fig. 1, A). The pattern and intensity of TSP-3 staining in muscle was unaltered in *Thbs4*$^{-/-}$ mice (not shown). In tendons, TSP-4 and TSP-3 are associated with distinct

fibrillar structures. Similar to TSP-4, TSP-5 is found in the perimysium of muscle and in tendon (Fig. 1, B–D). The staining of TSP-5 overlaps extensively with TSP-4 staining (Fig. 1, B, C) in WT mice. However, the intensity of TSP-5 staining in tendon was not changed in *Thbs4*$^{-/-}$ mice (Fig. 1, D). Western blotting of extracts of skeletal muscle (soleus) revealed that both TSP-3 and TSP-5 are present in the skeletal muscle tissue at low levels, and their expression is not altered (Suppl. Fig. 1). TSP-1 and TSP-2 were also expressed at the levels comparable to the expression levels in WT mice.

Immunohistochemical analysis of transverse sections of the patellar tendon demonstrated that TSP-4 is abundant (Fig. 1E, left panel). Specificity of the anti-TSP-4 antibody was demonstrated by the absence of any reactivity in the patellar tendon of *Thbs4*$^{-/-}$ mice (Fig. 1E, right panel) or in any other tissue derived from these animals (Frolova et al., 2010; Frolova et al., 2012), and the absence of the protein as detected by Western blotting (Fig. 6A and 8C). The abundant expression of TSP-4 in the tendon suggests its potential importance in the organization of this tissue.

2.3. TSP-4 regulates the structure of the collagen fibrils in tendon

Patellar tendons were harvested, and collagen fibers were imaged by transmission electron microscopy (TEM). The morphological analysis of transverse sections of patellar tendons demonstrated that the distribution of the areas and diameters of the collagen fibrils were different in WT and *Thbs4*$^{-/-}$ mice (Fig. 2, A). In the *Thbs4*$^{-/-}$ mice, fibril areas (Fig. 2, B) and fibril diameters (Fig. 2, C) were more variable, and larger fibrils were over-represented (Fig. 2, B, C). Fibril area distribution in WT tendon has two readily discernable peaks centered at ~ 0.0050 μm^2 and ~0.0230 μm^2. The two peaks of fibril area in *Thbs4*$^{-/-}$ tendon were less pronounced, broader and shifted toward larger fibril areas with peaks at ~ 0.0072 μm^2 and at 0.028 μm^2. (Fig. 2, B). The population of fibers with areas greater than 0.035 μm^2 comprised 16% of all fibers in *Thbs4*$^{-/-}$ tendon, but less then 1% in the WT mice. In *Thbs4*$^{-/-}$ tendon, the larger population of fibers had diameters centered around ~200 nm, whereas in the WT tendons, the larger population of fibers had diameters centered around ~160 nm (Fig. 2, C). All the differences were statistically significant ($p<0.05$, $n\geq5$). Despite this shift in size distribution, the shapes of fibrils were not altered in tendons of *Thbs4*$^{-/-}$ mice; WT and *Thbs4*$^{-/-}$ fibrils were similar in aspect ratios (Fig. 2, D).

2.4. Distribution of TSP-4 in WT muscle

TSP-4 expression was reported in myotendinous junctions and in the perimysium of muscles(Arber and Caroni, 1995). We found that TSP-4 expression is not limited to the perimysium but is also abundant in the endomysium of muscles (Fig. 3, A–E). TSP-4 was detected in a close proximity to every fiber in the soleus, where the fibers are predominantly type I (slow oxidative) (Fig. 3, B). TSP-4 was also found around some but not all fibers in the gastrocnemius. These fibers are type I (slow oxidative) and type IIa (fast oxidative), as revealed by comparison with parallel muscle sections stained for the activity of succinate dehydrogenase, an enzyme involved in oxidative phosphorylation and immunostaining for the myosin type (not shown). Immunostaining revealed only modest staining for TSP-4 in a punctate pattern in the white portion of the muscle, which consists of type IIb fibers (Fig. 3, C, E).

Previously, we reported that TSP-4 is expressed by endothelial cells and smooth muscle cells in the walls of blood vessels (Stenina et al., 2003). To determine whether TSP-4 in skeletal muscle tissue is also found in association with the microvessels adjacent to the muscle fibers, we injected FITC-conjugated *Lycopersicon esculentum* lectin, which binds specifically to endothelial cell membranes (Hansen-Smith et al., 1992), into WT and *Thbs4*$^{-/-}$ mice and co-stained the sections with anti-TSP-4 antibodies. TSP-4 localized in close proximity to endothelial cells on the basal side of endothelium (Fig. 3, F).

2.5. Extracellular matrix in soleus of *Thbs4*$^{-/-}$ mice

ECM was visualized by Masson trichrome staining of soleus sections (Fig. 3G–J). The area of deposition of ECM was quantified in the muscle of WT and *Thbs4*$^{-/-}$ mice using ImagePro 6.1 as described in our previous reports (Frolova et al., 2010; Frolova et al., 2012). There was no change in gastrocnemius, where TSP-4 was poorly expressed. However, a significant decrease of ECM was detected in soleus, where TSP-4 is abundant (Fig. 3K).

2.6. Comparison of TSP-4 to TSP-3 and TSP-5 expression in blood vessels of muscle

We have visualized blood vessels of muscle by staining endothelial cells using FITC-conjugated lectin from *Lycopersicon esculentum* or anti-vWF antibody. TSP-4 was detected in arteries, veins and capillaries but its expression was discontinuous: regions rich in TSP-4 and region lacking TSP-4 were present in each type of vessel. To compare the distribution and localization of all the homologous TSPs of subgroup B, we stained blood vessels with antibodies against TSP-3 and TSP-5. While all three TSPs were detected in small arteries, they did not co-localize (Fig. 4, A–J). TSP-4 was abundant in capillaries, but there was no TSP-5 or TSP-3 expression in the capillaries. Thus, while all three TSPs can be present in arterial wall and both TSP-4 and TSP-3 are found in veins, they do not co-localize and there is no evidence for compensation of TSP-4 deficiency. TSP-5 expression was observed along the basal membrane of the muscle fibers (Fig. 4, K and L), whereas TSP-4 expression was detected in the space between fibers, its expression was restricted to the capillaries.

2.7. TSP-4 and heparan sulfates in the muscle

All TSP family members have heparin-binding sites (Adams, 2001; Chen et al., 2007), and certain functions of the TSPs may be dependent on their interactions with glycosaminoglycans (GAGs). Heparan Sulfates (HS) are present in the ECM, in the basal lamina and on the cell membranes, and are known to be involved in wide variety of cellular functions (Jenniskens et al., 2006). On this basis, we postulated that the absence of TSP-4 might affect the structure of specific HS in *Thbs4*$^{-/-}$ mice. Accordingly, immunostaining was performed with antibodies to six distinct HS epitopes (Dennissen et al., 2002; Jenniskens et al., 2000; van Kuppevelt et al., 1998) that report on different unidentified modifications of HS chains (Fig. 5 and Suppl. Fig. 2). Of the six HS epitopes analyzed, the three recognized by antibodies HS3B7, RB4CB9, and EV3C3, showed decreased presence in the soleus of *Thbs4*$^{-/-}$ mice compared to WT (Fig. 5, A). In WT mice, these three epitopes either overlapped with TSP-4 staining or were detected in close proximity to TSP-4 (Fig. 5B–D). The effect of TSP-4 deficiency on the presence of GAG epitopes was selective

as no difference in the expression of three other HS epitopes, A4BO8, HS4C3, RB4CB12 (Suppl. Fig. 2), was observed.

2.8. HS core proteins in soleus and cultured microvascular endothelial cells (EC) from *TSP-4*$^{-/-}$ mice

Specific HS core proteins (syndecan, glypican, perlican) as well as total Heparan Sulfates were detected in the soleus tissue and in microvascular EC from WT and *Thbs4*$^{-/-}$ mice by Western blotting (Fig. 6). Equal loading was routinely monitored by staining the membranes with Ponceau Red before immediately after the transfer (before incubations with primary antibodies) and by staining the membranes with Coommassie Blue after completion of the experiment. Perlican could not be detected (not shown). Syndecan levels were not changed in the tissue, but more of this protein was detected on the surface of the EC from *Thbs4*$^{-/-}$ mice and in whole EC lysates. Glypican was remarkably absent for the muscle tissues of *Thbs4*$^{-/-}$ mice, but was expressed at the higher levels on the surface of cultured EC cells. In addition to glypican, another HS protein of MW ~130 kD was completely missing from the muscle tissues of *Thbs4*$^{-/-}$ mice. Based on the MW, we have analyzed the expression of beta-glycan, a receptor for TGFβ, and found that beta-glycan was indeed significantly downregulated in muscle tissue and cultured EC from *Thbs4*$^{-/-}$ mice (Fig. 6B). Addition of 10 μm rTSP-4 to the culture media increased the production of beta-glycan in cultured microvascular EC. To understand how the decreased expression of beta-glycan affects TGFβ-related signaling, we examined phosphorylation of p38 and smad2, two main intracellular mediators of TGFβ signaling. Both pathways were activated more in cells and tissues from *Thbs4*$^{-/-}$ mice, suggesting that beta-glycan normally plays inhibitory role, and this function is lost in *Thbs4*$^{-/-}$ mice.

2.9. Levels of HS-synthesizing enzymes in cultured microvascular EC from *TSP-4*$^{-/-}$ mice

Changes in expression of HS core proteins both in the lysates and on the surface of cultured EC suggested that TSP-4 influences their expression rather than their retention in tissues. Western blotting of lysates of microvascular EC isolated from WT and *TSP-4*$^{-/-}$ mice with antibodies against heparan sulfate 2-O-sulfotransferase 1 and N-heparan sulfate sulfotransferase 3, two enzymes controlling key steps in synthesis of HS (the initial chemical modifications required for the biosynthesis of the functional oligosaccharide sequences that define the specific ligand binding activities of HS), revealed the decreased levels of both enzymes in EC from *TSP-4*$^{-/-}$ mice and stimulation of their expression by rTSP-4 added to the cell culture media (Fig. 6C).

2.10. Uptake of very low density lipoproteins (VLDL) by endothelial cells of *TSP-4*$^{-/-}$ mice

The binding and activity of many proteins and lipoproteins depends on surface of EC depends on the composition of GAGs (Kolset and Salmivirta, 1999). Specific modifications of GAGs are recognized by antithrombin (De Agostini et al., 1990; Naimy et al., 2008; Rosenberg and de Agostini, 1992), Fibroblasts growth factor 2 (FGF2)(Ye et al., 2001) and lipoprotein lipase (LPL)(Misra et al., 1994; Parthasarathy et al., 1994; Shimada et al., 1981). Furthermore, LPL is active only when bound to the cell surface GAGs (Berryman and Bensadoun, 1995; Eisenberg et al., 1992; Fuki et al., 2003; Rumsey et al., 1992; Williams et

al., 1992). We have evaluated the uptake of VLDL, which is dependent on lipoprotein lipase activity (the rate limiting enzyme for hydrolysis of lipoprotein triglyceride that also mediates nonenzymatic interactions between lipoproteins and heparan sulfate proteoglycans), in EC derived from *Thbs4*$^{-/-}$ and WT mice and *in vivo* in soleus of *Thbs4*$^{-/-}$ and WT mice. The uptake of DiI-VLDL was significantly reduced in cultured EC of *Thbs4*$^{-/-}$ mice (Fig. 7, A and B) and in the skeletal muscle of *Thbs4*$^{-/-}$ mice (Fig. 7C). The decreased uptake of VLDL (Fig. 7) and the decreased levels of GAGs (Fig. 5) suggests that TSP-4 may regulate lipoprotein lipase activity by affecting the composition of ECM and cell surface GAGs.

2.11. LPL levels and activity in *Thbs4*$^{-/-}$ mice

LPL activity was measured in cultured EC isolated from *Thbs4*$^{-/-}$ and WT mice (Fig. 8A). The activity of endothelial LPL was also evaluated *in vivo* in *Thbs4*$^{-/-}$ and WT mice (Fig. 8B). In both models, the activity of LPL was reduced in the *Thbs4*$^{-/-}$ mice. The expression of LPL was analyzed by Western blotting (Fig. 8C). More LPL protein was detected both in the extracts of muscle tissues from *TSP-4*$^{-/-}$ mice and in the lysates and on the surface of EC from *TSP-4*$^{-/-}$ mice, suggesting that the loss of activity could not be explained solely by the decreased levels of LPL.

2.12. Metabolic changes in *Thbs4*$^{-/-}$ mice

Impaired release of free fatty acids from VLDL may lead to global metabolic changes associated with the decreased uptake of free fatty acids by skeletal muscles (e.g., the metabolism of energy in the skeletal muscle may rely more on glucose uptake and metabolism leading to global changes in metabolic indeces). We have measured blood glucose, insulin, LDL, HDL, non-esterified fatty acids (NEFA, free fatty acids), and VLDL in WT and *Thbs4*$^{-/-}$ mice at 8, 20 and 35 weeks (Table 1). No difference was detected in levels of LDL, HDL, NEFA or cholesterol between two strains of mice. However, glucose levels in the blood of *Thbs4*$^{-/-}$ mice were altered as early as 8 weeks and it remained consistently lower in fasting mice of older ages. Difference in insulin levels (lower levels in *Thbs4*$^{-/-}$ mice) became statistically significant at 20 weeks of age. At 8 weeks, difference in NEFA levels was detected in mice that received oil gavage: the blood levels of NEFA were lower in *Thbs4*$^{-/-}$ mice. Significantly lower levels of NEFA were detected in older mice of 55 weeks of age without oil gavage. To test whether the subtle alteration may become overt in mice on the high fat/high carbohydrate content, we kept groups of mice on the high fat/high carbohydrate diet starting at age 4 weeks. In addition to differences in blood glucose and insulin, mice on the high fat/high carbohydrate content diet developed higher blood levels of total cholesterol and VLDL, consistent with the inability to process VLDL dues to the impaired function of endothelial LPL.

2.13. Altered mass of skeletal muscle of *Thbs4*$^{-/-}$ mice

Muscles from male and female WT and *Thbs4*$^{-/-}$ mice were dissected and weighed. There was no difference in the weights of gastrocnemius of WT and *Thbs4*$^{-/-}$ mice: e.g., at 29 weeks, the weight of gastrocnemius was 75±6 mg/cm in *Thbs4*$^{-/-}$ mice vs 73±3 mg/cm in WT males (n=8, p=0.28). However, the weight of the soleus was altered in *Thbs4*$^{-/-}$ mice starting as early as at 8 weeks of age.

At 8–14 weeks of age, the soleus from *Thbs4*$^{-/-}$ animals had ~ 30% less mass compared to WT mice (2.75±0.37 mg/cm in *Thbs4*$^{-/-}$, n =10, versus 3.89±0.27 mg/cm in WT, n=4, $p<0.05$, males, weight normalized per tibia length) (Fig. 9, A). Differences in the weight of the soleus were sustained from 29 to 50 weeks and continued in older mice [75 weeks of age (2.21±0.5 mg/cm in *Thbs4*$^{-/-}$ mice, n =4, versus 4.1±0.65 mg/cm in WT, n = 5, $p<0.05$)]. The soleus of female mice tended to be smaller in *Thbs4*$^{-/-}$ versus WT as well; at 72 weeks of age, 4.1±0.5 mg/cm in *Thbs4*$^{-/-}$ mice versus 5.34±0.39 mg/cm in WT, n = 4 for both groups, $p<0.05$. Examination of the microstructure of the soleus from *Thbs4*$^{-/-}$ mice revealed that the individual the lack of adhesion between the fibers (Fig. 9, B), consistent with the loss of ECM (Fig. 3H–K). While anecdotal, we found that the soleus muscles from *Thbs4*$^{-/-}$ mice were more fragile and difficult to section than the same tissue derived from WT mice. The size of myocytes was not changed, suggesting that the altered weight and function of the muscles were due to the loss of ECM and resulting functional changes.

2.14. Altered function of limbs in *Thbs4*$^{-/-}$ mice

To determine whether the abnormal tendon structure and the biochemical changes in skeletal muscle translate into a dysfunction of the whole limb, we examined whether the lack of TSP-4 and its influence on muscle mass affected the strength of *Thbs4*$^{-/-}$ mice. The strength of the front and hind limbs of mice of both genders at different ages was measured using a dynamometer. The average grip strength in younger mice (<6 week old) was nearly identical in both groups of animals in both genders (Fig. 9, C; $p = 0.86$). Average strength decreased modestly in *Thbs4*$^{-/-}$ mice starting at the 7th week of age, and continued to decrease markedly by 76–82 weeks compared to WT mice (Fig. 9, C). This observation suggests that, compared to WT mice, *Thbs4*$^{-/-}$ mice are less capable of maintaining grip strength with age thereby implying possible impairment of muscle function.

3. DISCUSSION

In this work, we have examined the effect of TSP-4 deletion on the structure of tendon and muscle and on the performance of the whole limb in *Thbs4*$^{-/-}$ mice. We found profound changes in the structure of tendon and in the composition of red muscle ECM, which translated into the impaired metabolism of the main source of energy of the red muscle (VLDL) and in altered intracellular signaling. The major findings of our study are: 1) TSP-4 controls the deposition of ECM in tendon and skeletal muscle; 2) TSP-4 is necessary for the correct organization of collagen fibrils in tendon; 3) The expression of TSP-4 in skeletal muscle is associated with fibers relying on oxidative metabolism, and TSP-4 is necessary to maintain the uptake of fatty acids from VLDL; 4) The effects of TSP-4 on skeletal muscle structure and metabolism are, at least in part, mediated by controlling the correct HS modification; and 5) The function of the whole limb is affected by the changes in tendon and skeletal muscle structure and function.

Similar to mice with deficiencies of the other two members of TSP subgroup B (Hankenson et al., 2005; Svensson et al., 2002), *Thbs4*$^{-/-}$ mice do not show obvious anatomical or functional differences compared to WT mice. However, when *Thbs4*$^{-/-}$ mice are challenged in disease models that affect the organs with the highest level of TSP-4 expression (e.g., heart (Cingolani et al., 2011; Frolova et al., 2012; Lynch et al., 2012) and blood vessels

(Frolova et al., 2010; Mustonen et al., 2008), the role of TSP-4 as regulator of ECM and cell-matrix interactions are readily discerned. In the models of pressure overload, TSP-4 was necessary to control fibrosis of myocardium and to prevent excessive ECM deposition leading to heart hypertrophy and abnormal function of cardiomyocytes and the whole myocardium.

On closer examination of *Thbs4*$^{-/-}$ mice, structural and/or functional abnormalities were found in tendon and skeletal muscle, two tissues that display abundant TSP-4 expression in WT mice. Tendon was known as a tissues with abundant expression of TSP-4 (Hauser et al., 1995; Hecht et al., 1998; Sodersten et al., 2006), TSP-1 (Kannus et al., 1998), TSP-2 (Kyriakides et al., 1998) and TSP-5 (Hecht et al., 1998). Our data add TSP-3 to this list. Thus, mouse tendon expresses all five TSP family members. In tendon of *Thbs4*$^{-/-}$ mice, collagen fibers are abnormal in size and organization. TEM analysis of patellar tendon revealed alterations in the size of collagen fibers. The most noticeable change was the increased number of larger fibers in *Thbs4*$^{-/-}$ patellar tendon. Deficiencies of several other matrix proteins, including thrombospondin-2 (Kyriakides et al., 1998), decorin (Zhang et al., 2006), lumican (Jepsen et al., 2002), collagen type V (Marchant et al., 1996), fibromodulin (Ezura et al., 2000) and biglycan (Ameye et al., 2002; Corsi et al., 2002) are associated with alterations in the diameter of collagen fibrils in various tissues, including patellar tendon. The alteration in fiber diameter in *Thbs4*$^{-/-}$ patellar tendon is similar to that observed in the FDL (*flexor digitorum longus*) tendon in decorin-deficient mice, where an increased number of larger diameter fibers was observed. Also, of note, larger collagen fibrils were observed in the patellar tendon of *Thbs2*$^{-/-}$ mice. However, in *Thbs2*$^{-/-}$ mice, tail tendons were lax, and both ligaments and skin were fragile (Kyriakides et al., 1998). Such manifestations of collagen disorganization were not observed in the *Thbs4*$^{-/-}$ mice, although the changes in fibril size and in their organization clearly indicate that TSP-4 is required for the correct fibril assembly and likely for their interaction with other ECM proteins and/or the maintenance of the correct composition of the ECM in tendon.

In WT muscle, TSP-4 expression is detected in the perimysium and in the endomysium and is especially abundant in red muscles. ECM levels are affected by TSP-4 deficiency in soleus (red muscle): the amount of ECM is decreased ~40% in soleus of *Thbs4*$^{-/-}$ mice, but not in gastrocnemius. This decrease in ECM production or retention is in contrast with the effect of TSP-4 on ECM in myocardium, where the deficiency in TSP-4 results in increased production of ECM and increased size of the heart. Although the mechanisms of ECM regulation in both organs are unknown, it is clear that the effects of TSP-4 on ECM production and composition are organ-specific. Our results demonstrate that TSP-4 is required for the correct modification, production and/or retention of several heparan sulfate proteoglycans in skeletal muscle. TSP-4 expression is associated with different types and sizes of blood vessels in the muscle. When present, it is localized primarily to the tunica adventitia in larger vessels or on the basal side of endothelium in capillaries.

TSP-4 shares up to 82% homology with TSP-3 and TSP-5 in C-terminal part and may be able to form heteromers with TSP-5 (Hecht et al., 1998; Sodersten et al., 2006). Therefore, we considered whether another subgroup B family member might substitute for TSP-4. Such substitution and compensation of functions would be suggested by the similarity in

localization and increase in levels of TSP3 and/or TSP5 in *Thbs4*$^{-/-}$ mice. All three TSP subgroup B members are expressed in tendon, skeletal muscle and blood vessels, but the patterns of their distributions in these tissues are distinct. TSP-5 had been previously demonstrated to be present in blood vessels (Riessen et al., 2001), but this localization had not been reported for TSP-3. The absence of TSP-4 in *Thbs4*$^{-/-}$ mice did not alter the intensity or distribution of other two highly homologous family members of subgroup B in blood vessels, suggesting that the functions of TSP-4 are different from the functions of TSP-3 and TSP-5, and TSP-4 deficiency is not compensated. Although we found TSP-3 to be expressed in tendon, it is associated with different tendon structures than TSP-4 or TSP-5. TSP-5 is also expressed in tendon, and its expression overlaps with that of TSP-4. However, based on our careful examination of the two molecules using immunohistochemistry/confocal microscopy and Western blotting of the extracts from soleus, we did not detect any increase in the expression of TSP-5 or TSP-3 in tendon of *Thbs4*$^{-/-}$ mice. Based on the detection in Western blotting, there was no compensatory overexpression of any of four other TSPs in skeletal muscle tissues.

All TSPs, including TSP-4, have heparin-binding sites (Chen et al., 2007; Narouz-Ott et al., 2000) and interact with HS, which are ubiquitously distributed in the ECM and on cell surfaces, and are involved in the structural integrity of skeletal muscle ECM, the continuity between muscle ECM and tendon and, as a result, directly affect the function of tendons and muscles and the limb in whole. Using unique antibodies that recognize distinct but unidentified epitopes of GAGs (Dennissen et al., 2002; Jenniskens et al., 2000; van Kuppevelt et al., 2001), we found that TSP-4 influences the distribution of specific GAG epitopes in muscle. Our findings point to a selective interrelationship between TSP-4 and HS. TSP-4 co-localized with HS modifications recognized by the antibodies EV3C3, HS3B7, RB4CD9, but did not change the distribution of HS modifications recognized by the antibodies A4BO8, HS4C3V, RB4CB12. HSPGs are important for the structural integrity and proper function of the endothelium. HSPGs located on the basal side of vessels interact with a variety of basement membrane proteins (Hayashi et al., 1992). Basal HSPGs inhibit smooth muscle cell proliferation and migration (Castellot et al., 1981) and regulate processes of filtration in the endothelium (Kanwar and Farquhar, 1979). Thus, processes of nutrient exchange between the endothelium and muscle cells could be impaired with the loss of TSP-4 because of changes in the composition and/or amount of HS. We have identified altered levels of two HS core proteins in the muscle tissues of *TSP-4*$^{-/-}$ mice: loss of glypican and beta-glycan. Loss of beta-glycan was confirmed using cultured microvascular EC from *TSP-4*$^{-/-}$ mice and was associated with increased activity of two mediators of main pathways of TGFβ signaling (p38 and smad2) both in the tissues and in cultured EC. The role of beta-glycan as a TGFβ receptor is controversial: both activating and inhibiting activities on TGFβ have been ascribed (Bilandzic and Stenvers, 2011; Gatza et al., 2010). Our data suggest that beta-glycan has inhibiting effect on TGFβ signaling in skeletal muscle, and TSP-4 is required for its production/retention in the ECM. The decreased expression of two key enzymes controlling HS synthesis and modification and the restoration of their expression by rTSP4 suggests that TSP-4 affects the intracellular synthesis and correct modification of HS and, as a result, the levels of specific HS proteoglycans, including beta-glycan.

Many plasma proteins bind to the cell surface using distinct specific modifications and combinations of surface GAGs (De Agostini et al., 1990; Kolset and Salmivirta, 1999; Misra et al., 1994; Naimy et al., 2008; Parthasarathy et al., 1994; Rosenberg and de Agostini, 1992; Shimada et al., 1981; Ye et al., 2001). Based on our observation that TSP-4 is highly expressed in red muscle that utilizes primarily oxidative metabolism and that in *Thbs4*$^{-/-}$ mice these muscles are affected more than white muscles that utilize primarily glycolytic metabolism, we tested the activity of LPL, an endothelial enzyme responsible for the uptake and hydrolysis of lipoproteins (Berryman and Bensadoun, 1995; Eisenberg et al., 1992; Fuki et al., 2003; Rumsey et al., 1992; Williams et al., 1992). LPL becomes active upon binding to the EC surface by interacting with GAGs. We found that the uptake of VLDL and the activity of endothelial LPL were decreased in *Thbs4*$^{-/-}$ mice. Although the activity of LPL was reduced in both the tissues of soleus and in cultured EC, the levels of production of LPL were not decreased but rather increased in *Thbs4*$^{-/-}$ mice, and more LPL was associated with the cell surface. These observations suggest that LPL in *Thbs4*$^{-/-}$ mice is less active, probably as a result of incorrect binding to the surface due to the changes in HS composition, which does not support the enzyme activity. These relationships suggest a role of TSP-4 in maintenance of LPL activity by supporting production and modification of specific HS and, as a result, in the metabolism of red muscle.

The weight of the soleus muscle was decreased in *Thbs4*$^{-/-}$ mice as compared to WT. The loss in weight of older *Thbs4*$^{-/-}$ mice may be due to the reduction of red muscle mass in these animals. We also noticed that *Thbs4*$^{-/-}$ mice have higher blood levels of lactate, especially in older mice (data not shown), which suggests a perturbation of energy metabolism in muscle. Microscopic examination revealed alterations of structure consistent with altered ECM: lack of ECM or loss of ECM during the preparation of the section and loss of attachment between individual muscle fibers in *Thbs4*$^{-/-}$ mice. We attributed these changes to the loss of ECM, because the diameter of myocytes was not changed, and the staining of ECM revealed lower levels of ECM in *Thbs4*$^{-/-}$ mice.

Based on these structural changes in the skeletal muscle, abnormal tendon structure and decreased availability of energy supply from lipoproteins, we expected to find a decline in muscle mass and performance of the whole limb. Indeed, *Thbs4*$^{-/-}$ mice have less muscle strength than WT mice.

Taken together, these observations indicate a role of TSP-4 in the organization and functions of tendons, muscles and blood vessels, which translate into functional differences at the cellular level and differences in performance of the whole limb between *Thbs4*$^{-/-}$ and WT mice.

4. EXPERIMENTAL PROCEDURES

4.1

***Thbs4*$^{-/-}$ mice** have been described previously (Frolova et al., 2010; Frolova et al., 2012). In this study, we used mice that had been backcrossed for at least 8 generations with C57BL/6 mice. As controls, wild-type (WT) littermates or WT age-matched litters of

brother and sister matings were used. Genotyping was verified by PCR with primers that distinguish between the wild-type and the mutant allele. The primers used are:

GGAGAGAGAATAGCAAGATCAGCTC: gene-specific endogenous;

AACAAGCAATGGAAGGCAGACCCTG: gene-specific, endogenous and targeted;

GGGTGGGATTAGATAAATGCCTGCTCT:Neo, targeted.

The absence of TSP-4 mRNA and protein was confirmed by Northern and Western blots as well as by specific immunostaining of multiple tissues with anti-TSP-4 antibody (Frolova et al., 2010; Frolova et al., 2012). The mice were housed in the Biological Resource Unit in a temperature-controlled environment with a 12:12-h light-dark cycle and were fed a standard chow diet *ad libitum*. All animal procedures were performed according to NIH guidelines under protocols approved by the Institutional Animal Care and Use Committee of the Cleveland Clinic.

4.2. Antibodies

The TSP-4 antibody used (R&D, Minneapolis, MN) was raised in a goat using a part of the TSP-4 molecule that is homologous between human and mouse (Ala22-Asn961), and it recognized both human and mouse TSP-4. Rabbit anti-TSP-3 IgG was from Santa Cruz (Santa Cruz, CA). Rat anti-COMP (TSP-5) IgG was from Affinity BioReagents (Golden, CO). Antibodies to specific GAG modifications have been previously described (Dennissen et al., 2002; Jenniskens et al., 2000; van Kuppevelt et al., 2001). For immunohistochemistry, the periplasmic fractions containing VSV-tagged single chain antibodies, designated HS3B7 *(epitope preference not known)*, RB4CB9 *(IdoA, NS (inhibitory: 2OS, 6OS))*, EV3C3 *(epitope preference not known)*, RB4CD12 *(NS, 2OS, 6OS [IdoA2S-GlcNS6S])*, AO4BO8 *(IdoA, NS, 2OS, 6OS [IdoA2S-GlcNS6S])*, HS4C3 *(NS, 3OS, 6OS [IdoA2S-GlcNS3S6S])* were used. Polyclonal rabbit anti-VSV IgG from MBL (Woburn, MA) and Alexa 488-labeled anti-rabbit IgG (Molecular Probes, Eugene, OR) were used for their detection. Other secondary antibodies, Rhodamine Red-X anti-goat IgG, Rhodamine Red-X anti-rabbit IgG, Rhodamine Red-X anti-rat IgG, FITC anti-rabbit IgG were from Jackson ImmunoResearch (West Grove, PA), Alexa 488 anti-goat IgG was from Invitrogen/Life technologies (Grand Island, NY). Anti-CD31 antibody was from BD Biosciences (San Jose, CA). Anti-beta-glycan, anti-phospho-SMAD2, and anti-phospho-p38 antibodies were from Cell Signaling Technology (Beverly, MA), anti-NDST1 and anti-HS2ST1 antibodies were from MyBiosource (San-Diego, CA), anti-LPL antibody was from LSBio (Seattle, WA), anti-TSP1 was from LabVision/Neo Markers (mouse ab-4, Fremont, CA), anti-TSP2 antibody was from R&D Systems (Minneapolis, MN), anti-glypican antibody was from Proteintech (Chicago, IL), anti-perlican antibody was from Acris Antibodies (San Diego, CA), anti-syndican antibody was from Abcam (Cambridge, MA), and anti-Heparan Sulfate antibody was from AMSBio (Lake Forest, CA).

4.3. Immunohistochemistry

Mice were sacrificed by CO_2 inhalation followed by cervical dislocation; triceps were harvested and placed on 7% Gum Tragacanth (Sigma, St. Louis, MO), frozen in liquid nitrogen-cooled isopentane (Sigma, St. Louis, MO) and stored at −80°C until processing.

Frozen sections (10–12 μm) were cut in a cryostat (Leica, Wetzlar, Germany) and placed on microscope slides (Superfrost; Fisher Scientific, Waltham, MA). Sections were immediately blocked by incubation in PBS containing 5% BSA (MB Biomedicals, OH) and donkey IgG (1:50) for 30 min at 4°C. Following this treatment, the slides were incubated with primary antibodies for 2 h at 4°C. The concentrations of the primary antibodies used were as follows: rabbit anti-TSP-3: 1:50; goat anti-TSP-4: 1: 200; anti-TSP-5: 1: 10. After washing with PBS/BSA (3x10 min), primary antibodies were detected by incubating sections in Rhodamine Red-X (1:200) or FITC (1:100)-conjugated secondary antibodies for 45 min at 4°C. For double immunofluorescence labeling using antibodies to TSP-4 and TSP-3 or TSP-5, the two primary and secondary antibodies were applied to the sections simultaneously. For double-labeling sections for TSP-4 and GAG epitopes, cryosections of transverse triceps were first blocked and then incubated with the periplasmic fraction containing the selected single chain antibody (1:1–1:5) for 1.5 h. After three washes in PBS/BSA, the anti-VSV antibody (1:100–1:500 diluted with PBS/BSA) and anti-TSP-4 was added for 1 h followed by detection with FITC-conjugated anti-rabbit IgG (1:200) and Rhodamine Red-X anti-goat IgG. Sections were mounted in Vectashield with DAPI (Vector Lab. Inc., Burlingame, CA).

4.4. Confocal Microscopy

Z-stacks of images were collected using a Leica TCS-SP3-AOBS Laser Scanning Confocal Microscope (Leica Microsystems Inc., Bannockburn, IL) with an HCX Plan Apo 40x/1.25 NA oil immersion objective. All z-series were collected using the same number of slices, step size (0.4 μm), and collection parameters including brightness, contrast and pinhole. Image stacks from the z-series were reconstructed and analyzed using Volocity 4.1.0 software (Improvision Inc., Lexington, MA). Matching areas from WT and *Thbs4*$^{-/-}$ samples (WT, n=5; *Thbs4*$^{-/-}$, n=5), which excluded tendons and blood vessels, were selected for analysis. The mean integrated optical density (IOD) was calculated from selected areas for comparison between WT and *Thbs4*$^{-/-}$ samples.

4.5. Transmission Electron Microscopy

Three male and three female mice of WT (C57/BL6) or *Thbs4*$^{-/-}$ genotypes were analyzed. Following sacrifice ~ 2 × 3 mm of the central region of the patellar tendons was dissected and cleaned of loose connective tissue, the paratendon and epitendon. Tissues were immediately fixed in 2.5% glutaraldehyde/4% paraformaldehyde, pH 7.3, for 24 h, followed by postfixation with 1% osmium tetroxide for 1h. After *en bloc* staining and dehydration with a series of graded ethanol, the samples were embedded with eponate 12, polymerized at 68 °C for 48 h, trimmed, sectioned at 70–90 nm using a diamond knife on a Leica Ultramicrotome, and poststained in 50% saturated uranyl acetate and 0.2% lead citrate. The sections were examined and photographed at 60 kV using a Philips CM12 transmission electron microscope (FEI, Hillsboro, OR). Film images of the central region of the tendon of each mouse were taken (one per mouse), digitized on a MicroTek flatbed scanner. Morphometric fibril analysis was performed using Image Pro Plus 6.1 (Media Cybernetics, Silver Spring, MD). In total, 429 to 693 collagen fibers per group were analyzed to measure the frequency of differences in fibril diameters.

4.6. Morphometric Analysis of Collagen Fibrils

Fibril morphometric parameters including area, number, roundness, radius-ratio, aspect ratio (the ratio between the major axis and the minor axis of the ellipse equivalent to the object), perimeter, and mean separation were extracted from EM images using a semi-automated batch-processing routine generated for Image Pro Plus 6.1 (Media Cybernetics, Silver Springs, MD). For accurate segmentation of fibrils, image noise was removed using a median filter and local equalization, and rank filters were applied to enhance fibril contrast. Subsequently, touching fibrils were separated using modified watershed and seed-fill algorithms, and detected fibrils were thresholded using various size and shape delimiters to produce a binary fibril mask. To confirm whether fibrils were correctly segmented, pseudo-colored fibril outlines (generated from the fibril mask) were superimposed upon the original EM image allowing the software user (blinded observer) to add missing fibrils or remove incorrectly segmented fibrils. Fibril morphometric parameters were calculated in the final (user-modified) fibril mask and exported to Excel. Lastly, for analysis of fibril separation, Euclidean Distance Map (EDM) and skeletonized representations of the inverted fibril mask were multiplied together to produce an image containing medial separation lines (1 pixel wide) between adjacent fibrils with pixel gray values corresponding to fibril separation (distance of medial pixel to fibril border). These pixel values were summed, divided by the total number of skeletal pixels, and multiplied by 2 to report mean fibril separation. With all parameters exported, customized Excel scripts were used to pool morphometric indices for *Thbs4*$^{-/-}$ and WT groups, calculate ranges, means, and standard errors, and to create histograms for each parameter to examine population distributions within each group.

4.7. Measurement of grip muscle strength

The front limb grip strength was measured using a dynamometer (Chatillon Digital Force Gauge, DFIS 2, Columbus Instruments, Columbus, OH). The mouse was allowed to grasp a horizontal fore limb pull bar with both front paws, and gentle traction was applied to the tail; at the point when the mouse released the bar, grip strength was recorded (Smith et al., 1995). The mean grip strength from between six to eight trials per mouse was analyzed. To measure the hind limb grip strength, the forepaws were supported for stability with a horizontal fore limb pull bar while the hind limbs gripped an angled wire mesh. The mouse was pulled by its tail toward the mesh steadily until it let go (~3 sec). The mean pulling force from six to eight trials per mouse was analyzed.

4.8. Staining and analysis of capillaries

Mice were anesthetized with 100 μl of ketamine/xylazine solution (100 mg/kg and 20 mg/kg respectively), followed by injection into the heart through the diaphragm of FITC-conjugated lectin from *Lycopersicon esculentum* (Sigma, St. Louis, MO), 60 μg/25 g of body weight in 150–200 μl of PBS. Anesthetized mice were sacrificed by cervical dislocation in 10 min. Triceps were isolated, frozen, sectioned, and stained for TSP-4 as described above.

In order to detect the changes in the vascularity of the soleus and the white part of the gastrocnemius muscles between WT and *Thbs4*$^{-/-}$ mice, z-series were collected from the same location in the muscles with a Leica TCS-SP3-AOBS Laser Scanning Confocal

Microscope using an HC Plan Apo 20x/0.7 NA oil immersion objective. Image stacks from the z-series were reconstructed using Volocity software (Improvision Inc., Lexington, MA, USA). Matching areas from WT and *Thbs4*$^{-/-}$ two-dimensional images of the reconstructions were selected for analysis using Image Pro Plus 6.1 (Media Cybernetics, Inc., Silver Spring, MD, USA). Grayscale images of the lectin labeling were extracted from each reconstructed image and analyzed using Image Pro Plus 6.1 to determine the area of lectin labeling per total selected area.

4.9. Uptake of DiI-VLDL *in vivo*

Male WT and *Thbs4*$^{-/-}$ mice, 24-weeks of age, were injected with 100 μl (0.5 mg/ml) of DiI-VLDL (Kalen Biomedical, Montgomery Village, MD), in the retro-orbital sinus. After 30 min, the mice were sacrificed by isoflurane overdose and perfused with 10 ml PBS injected in the left heart ventricle. Tissues were collected and frozen in O.C.T. and processed for immunohistochemistry as described above to visualize TSP-4, CD31 and DiI-VLDL by microscopy.

4.10. Uptake of DiI-VLDL by cultured endothelial cells (EC)

Mouse lung EC were isolated from WT and *Thbs4*$^{-/-}$ mice as described (Mahabeleshwar et al., 2006). After EC reached confluency, they were incubated in EGM-2 medium without heparin or serum for 72 hours, washed twice with PBS, and DiI-VLDL (6 mg/ml in 0.5 ml of the medium supplemented with serum and heparin) was added. After 3 hours at 37°C, cells were washed twice with PBS containing 0.4% BSA, followed by three washes in PBS. The cells were lysed with 1% SDS in 0.1M NaOH for 1 hour with gentle shaking. Fluorescence was measured at an excitation wave length 520nm and an emission wave length of 580 nm. Each experiment was performed in triplicate. To visualize the uptake of DiI-labeled VLDL, EC were seeded onto chamber slides. When cells reached confluency, DiI-VLDL (6 mg/ml) was added under the conditions described above. At the end of the experiment, the cells were washed 3 times with PBS and fixed in 4% paraformaldehyde.

4.11. Measurement of Lipoprotein Lipase (LPL) activity

Confluent cultures of EC from WT and *Thbs4*$^{-/-}$ mice were incubated overnight with 60 μg/ml VLDL (Kalen Biomedical, Montgomery Village, MD) in serum- and heparin-free medium. After removing the medium, medium containing 10 U/ml heparin and 2% BSA was added for 40 min to induce release of cell-surface-bound LPL. The cells were lysed by sonication, and LPL in the cells treated with heparin and in untreated cells was compared.

To measure active endothelial LPL *in vivo*, blood plasma samples were collected from WT and *Thbs4*$^{-/-}$ mice before and 10 min after the injection of 20U of heparin. The amount of active LPL was calculated as a difference between the activity before and after the heparin injection. LPL activity in culture supernatants and plasma samples was measured using Roar LPL Activity kit (Roar Biomedical, Inc., New York, NY) according to the manufacturer's instructions.

4.12

Metabolic indeces (blood glucose, insulin, lipoproteins, cholesterol, non-esterified fatty acids) were measured as was previously described (Frolova et al., 2010).

4.12. Statistical analysis

All data are represented as means ± SE or SD as indicated. Significant differences between two groups were determined with using an unpaired Student's t-test. The significance level (p) was set at 0.05. *$p < 0.05$ versus control; and **$p < 0.001$ versus control are distinguished by the number of asterisks.

Supplementary Material

Refer to Web version on PubMed Central for supplementary material.

Acknowledgments

We thank John Peterson, Mei Yin (Imaging Core, LRI, Cleveland Clinic) for excellent technical assistance, Suneel Apte, (Department of Biomedical Engineering) for helpful discussions and Quteba Ebrahem (Department of Ophthalmic Research, Cole Eye Institute, Cleveland Clinic) for help with the technique and pilot experiments with lectin injections.

This work was supported by National Institutes of Health Grants 1R01 DK067532-01 (OSA) and 1R01HL117216 (EFP and OSA).

Abbreviations

TSP	thrombospondin
EGF	epidermal growth factor like domains
SNP	single nucleotide polymorphism
EC	endothelial cells
ECM	extracellular matrix
ES cell line	embryonic stem cell line
COMP	cartilage oligomeric matrix protein
GAG	glycosaminoglycan
HS	heparan sulfates
IOD	integrated optical density
TEM	transmission electron microscopy
FITC	fluorescein isothiocyanate
DAPI	4′,6-diamidino-2-phenylindole
LPL	lipoprotein lipase
VLDL	very low density lipoproteins

DiI-VLDL	1,1′-dioctadecyl- 3,3,3′,3′-tetramethylindocarbocyanine perchlorate-labeled VLDL

References

Adams JC. Thrombospondins: multifunctional regulators of cell interactions. Annu Rev Cell Dev Biol. 2001; 17:25–51. [PubMed: 11687483]

Adams JC. Functions of the conserved thrombospondin carboxy-terminal cassette in cell-extracellular matrix interactions and signaling. Int J Biochem Cell Biol. 2004; 36:1102–1114. [PubMed: 15094125]

Adams JC, Lawler J. Cell-type specific adhesive interactions of skeletal myoblasts with thrombospondin-1. Mol Biol Cell. 1994; 5:423–437. [PubMed: 7519904]

Adams JC, Lawler J. The thrombospondins. Int J Biochem Cell Biol. 2004; 36:961–968. [PubMed: 15094109]

Ameye L, Aria D, Jepsen K, Oldberg A, Xu T, Young MF. Abnormal collagen fibrils in tendons of biglycan/fibromodulin-deficient mice lead to gait impairment, ectopic ossification, and osteoarthritis. FASEB J. 2002; 16:673–680. [PubMed: 11978731]

Arber S, Caroni P. Thrombospondin-4, an extracellular matrix protein expressed in the developing and adult nervous system promotes neurite outgrowth. J Cell Biol. 1995; 131:1083–1094. [PubMed: 7490284]

Berryman DE, Bensadoun A. Heparan sulfate proteoglycans are primarily responsible for the maintenance of enzyme activity, binding, and degradation of lipoprotein lipase in Chinese hamster ovary cells. J Biol Chem. 1995; 270:24525–24531. [PubMed: 7592670]

Bilandzic M, Stenvers KL. Betaglycan: a multifunctional accessory. Mol Cell Endocrinol. 2011; 339:180–189. [PubMed: 21550381]

Bornstein P. Diversity of function is inherent in matricellular proteins: an appraisal of thrombospondin 1. J Cell Biol. 1995; 130:503–506. [PubMed: 7542656]

Bornstein P. Thrombospondins as matricellular modulators of cell function. J Clin Invest. 2001; 107:929–934. [PubMed: 11306593]

Castellot JJ Jr, Addonizio ML, Rosenberg R, Karnovsky MJ. Cultured endothelial cells produce a heparinlike inhibitor of smooth muscle cell growth. J Cell Biol. 1981; 90:372–379. [PubMed: 7287812]

Chen FH, Herndon ME, Patel N, Hecht JT, Tuan RS, Lawler J. Interaction of cartilage oligomeric matrix protein/thrombospondin 5 with aggrecan. J Biol Chem. 2007; 282:24591–24598. [PubMed: 17588949]

Chen H, Herndon ME, Lawler J. The cell biology of thrombospondin-1. Matrix Biol. 2000; 19:597–614. [PubMed: 11102749]

Cingolani OH, Kirk JA, Seo K, Koitabashi N, Lee DI, Ramirez-Correa G, Bedja D, Barth AS, Moens AL, Kass DA. Thrombospondin-4 is required for stretch-mediated contractility augmentation in cardiac muscle. Circ Res. 2011; 109:1410–1414. [PubMed: 22034490]

Corsi A, Xu T, Chen XD, Boyde A, Liang J, Mankani M, Sommer B, Iozzo RV, Eichstetter I, Robey PG, Bianco P, Young MF. Phenotypic effects of biglycan deficiency are linked to collagen fibril abnormalities, are synergized by decorin deficiency, and mimic Ehlers-Danlos-like changes in bone and other connective tissues. J Bone Miner Res. 2002; 17:1180–1189. [PubMed: 12102052]

Cui J, Randell E, Renouf J, Sun G, Green R, Han FY, Xie YG. Thrombospondin-4 1186G>C (A387P) is a sex-dependent risk factor for myocardial infarction: a large replication study with increased sample size from the same population. Am Heart J. 2006; 152:543, e541–545. [PubMed: 16923428]

Cui J, Randell E, Renouf J, Sun G, Han FY, Younghusband B, Xie YG. Gender dependent association of thrombospondin-4 A387P polymorphism with myocardial infarction. Arterioscler Thromb Vasc Biol. 2004; 24:e183–184. [PubMed: 15528485]

De Agostini AL, Lau HK, Leone C, Youssoufian H, Rosenberg RD. Cell mutants defective in synthesizing a heparan sulfate proteoglycan with regions of defined monosaccharide sequence. Proc Natl Acad Sci U S A. 1990; 87:9784–9788. [PubMed: 2263629]

Dennissen MA, Jenniskens GJ, Pieffers M, Versteeg EM, Petitou M, Veerkamp JH, van Kuppevelt TH. Large, tissue-regulated domain diversity of heparan sulfates demonstrated by phage display antibodies. J Biol Chem. 2002; 277:10982–10986. [PubMed: 11790764]

Eisenberg S, Sehayek E, Olivecrona T, Vlodavsky I. Lipoprotein lipase enhances binding of lipoproteins to heparan sulfate on cell surfaces and extracellular matrix. J Clin Invest. 1992; 90:2013–2021. [PubMed: 1430223]

Engel J. Role of oligomerization domains in thrombospondins and other extracellular matrix proteins. Int J Biochem Cell Biol. 2004; 36:997–1004. [PubMed: 15094115]

Ezura Y, Chakravarti S, Oldberg A, Chervoneva I, Birk DE. Differential expression of lumican and fibromodulin regulate collagen fibrillogenesis in developing mouse tendons. J Cell Biol. 2000; 151:779–788. [PubMed: 11076963]

Frolova EG, Pluskota E, Krukovets I, Burke T, Drumm C, Smith JD, Blech L, Febbraio M, Bornstein P, Plow EF, Stenina OI. Thrombospondin-4 regulates vascular inflammation and atherogenesis. Circ Res. 2010; 107:1313–1325. [PubMed: 20884877]

Frolova EG, Sopko N, Blech L, Popović ZB, Li J, Vasanji A, Drumm C, Krukovets I, Jain MK, Penn MS, Plow EF, Stenina OI. Thrombospondin-4 regulates fibrosis and remodeling of the myocardium in response to pressure overload. FASEB J. 2012 in press.

Fuki IV, Blanchard N, Jin W, Marchadier DH, Millar JS, Glick JM, Rader DJ. Endogenously produced endothelial lipase enhances binding and cellular processing of plasma lipoproteins via heparan sulfate proteoglycan-mediated pathway. J Biol Chem. 2003; 278:34331–34338. [PubMed: 12810721]

Gatza CE, Oh SY, Blobe GC. Roles for the type III TGF-beta receptor in human cancer. Cell Signal. 2010; 22:1163–1174. [PubMed: 20153821]

Gilsohn E, Volk T. Slowdown promotes muscle integrity by modulating integrin-mediated adhesion at the myotendinous junction. Development. 137:785–794. [PubMed: 20110313]

Hankenson KD, Hormuzdi SG, Meganck JA, Bornstein P. Mice with a disruption of the thrombospondin 3 gene differ in geometric and biomechanical properties of bone and have accelerated development of the femoral head. Mol Cell Biol. 2005; 25:5599–5606. [PubMed: 15964815]

Hansen-Smith F, Banker K, Morris L, Joswiak G. Alternative histochemical markers for skeletal muscle capillaries: a statistical comparison among three muscles. Microvasc Res. 1992; 44:112–116. [PubMed: 1386405]

Hauser N, Paulsson M, Kale AA, DiCesare PE. Tendon extracellular matrix contains pentameric thrombospondin-4 (TSP-4). FEBS Lett. 1995; 368:307–310. [PubMed: 7628627]

Hayashi K, Madri JA, Yurchenco PD. Endothelial cells interact with the core protein of basement membrane perlecan through beta 1 and beta 3 integrins: an adhesion modulated by glycosaminoglycan. J Cell Biol. 1992; 119:945–959. [PubMed: 1385448]

Hecht JT, Deere M, Putnam E, Cole W, Vertel B, Chen H, Lawler J. Characterization of cartilage oligomeric matrix protein (COMP) in human normal and pseudoachondroplasia musculoskeletal tissues. Matrix Biol. 1998; 17:269–278. [PubMed: 9749943]

Jenniskens GJ, Oosterhof A, Brandwijk R, Veerkamp JH, van Kuppevelt TH. Heparan sulfate heterogeneity in skeletal muscle basal lamina: demonstration by phage display-derived antibodies. J Neurosci. 2000; 20:4099–4111. [PubMed: 10818145]

Jenniskens GJ, Veerkamp JH, van Kuppevelt TH. Heparan sulfates in skeletal muscle development and physiology. J Cell Physiol. 2006; 206:283–294. [PubMed: 15991249]

Jepsen KJ, Wu F, Peragallo JH, Paul J, Roberts L, Ezura Y, Oldberg A, Birk DE, Chakravarti S. A syndrome of joint laxity and impaired tendon integrity in lumican- and fibromodulin-deficient mice. J Biol Chem. 2002; 277:35532–35540. [PubMed: 12089156]

Kannus P, Jozsa L, Jarvinen TA, Jarvinen TL, Kvist M, Natri A, Jarvinen M. Location and distribution of non-collagenous matrix proteins in musculoskeletal tissues of rat. Histochem J. 1998; 30:799–810. [PubMed: 9988347]

Kanwar YS, Farquhar MG. Presence of heparan sulfate in the glomerular basement membrane. Proc Natl Acad Sci U S A. 1979; 76:1303–1307. [PubMed: 155819]

Kato TYA, Murase Y, Hirashiki A, Noda A, Yamada Y. Specific gene polymorphisms could be risk factors for coronary artery disease in individuals with or without hypertention. Circulation (Suppl). 2003; 108:IV–712.

Kolset SO, Salmivirta M. Cell surface heparan sulfate proteoglycans and lipoprotein metabolism. Cell Mol Life Sci. 1999; 56:857–870. [PubMed: 11212344]

Kyriakides TR, Zhu YH, Smith LT, Bain SD, Yang Z, Lin MT, Danielson KG, Iozzo RV, LaMarca M, McKinney CE, Ginns EI, Bornstein P. Mice that lack thrombospondin 2 display connective tissue abnormalities that are associated with disordered collagen fibrillogenesis, an increased vascular density, and a bleeding diathesis. J Cell Biol. 1998; 140:419–430. [PubMed: 9442117]

Lawler J, Duquette M, Whittaker CA, Adams JC, McHenry K, DeSimone DW. Identification and characterization of thrombospondin-4, a new member of the thrombospondin gene family. J Cell Biol. 1993; 120:1059–1067. [PubMed: 8432726]

Lawler J, Sunday M, Thibert V, Duquette M, George EL, Rayburn H, Hynes RO. Thrombospondin-1 is required for normal murine pulmonary homeostasis and its absence causes pneumonia. J Clin Invest. 1998; 101:982–992. [PubMed: 9486968]

Lynch JM, Maillet M, Vanhoutte D, Schloemer A, Sargent MA, Blair NS, Lynch KA, Okada T, Aronow BJ, Osinska H, Prywes R, Lorenz JN, Mori K, Lawler J, Robbins J, Molkentin JD. A thrombospondin-dependent pathway for a protective ER stress response. Cell. 2012; 149:1257–1268. [PubMed: 22682248]

Mahabeleshwar GH, Somanath PR, Byzova TV. Methods for isolation of endothelial and smooth muscle cells and in vitro proliferation assays. Methods Mol Med. 2006; 129:197–208. [PubMed: 17085813]

Marchant JK, Hahn RA, Linsenmayer TF, Birk DE. Reduction of type V collagen using a dominant-negative strategy alters the regulation of fibrillogenesis and results in the loss of corneal-specific fibril morphology. J Cell Biol. 1996; 135:1415–1426. [PubMed: 8947562]

McCarthy JJ, Parker A, Salem R, Moliterno DJ, Wang Q, Plow EF, Rao S, Shen G, Rogers WJ, Newby LK, Cannata R, Glatt K, Topol EJ. Large scale association analysis for identification of genes underlying premature coronary heart disease: cumulative perspective from analysis of 111 candidate genes. J Med Genet. 2004; 41:334–341. [PubMed: 15121769]

Misenheimer TM, Mosher DF. Biophysical characterization of the signature domains of thrombospondin-4 and thrombospondin-2. J Biol Chem. 2005; 280:41229–41235. [PubMed: 16246837]

Misra KB, Kim KC, Cho S, Low MG, Bensadoun A. Purification and characterization of adipocyte heparan sulfate proteoglycans with affinity for lipoprotein lipase. J Biol Chem. 1994; 269:23838–23844. [PubMed: 8089154]

Mosher DF, Adams JC. Adhesion-modulating/matricellular ECM protein families: a structural, functional and evolutionary appraisal. Matrix Biol. 2012; 31:155–161. [PubMed: 22265890]

Murphy-Ullrich JE, Iozzo RV. Thrombospondins in physiology and disease: new tricks for old dogs. Matrix Biol. 2012; 31:152–154. [PubMed: 22265891]

Mustonen E, Aro J, Puhakka J, Ilves M, Soini Y, Leskinen H, Ruskoaho H, Rysa J. Thrombospondin-4 expression is rapidly upregulated by cardiac overload. Biochem Biophys Res Commun. 2008; 373:186–191. [PubMed: 18541142]

Naimy H, Leymarie N, Bowman MJ, Zaia J. Characterization of heparin oligosaccharides binding specifically to antithrombin III using mass spectrometry. Biochemistry. 2008; 47:3155–3161. [PubMed: 18260648]

Narouz-Ott L, Maurer P, Nitsche DP, Smyth N, Paulsson M. Thrombospondin-4 binds specifically to both collagenous and non-collagenous extracellular matrix proteins via its C-terminal domains. J Biol Chem. 2000; 275:37110–37117. [PubMed: 10956668]

Parthasarathy N, Goldberg IJ, Sivaram P, Mulloy B, Flory DM, Wagner WD. Oligosaccharide sequences of endothelial cell surface heparan sulfate proteoglycan with affinity for lipoprotein lipase. J Biol Chem. 1994; 269:22391–22396. [PubMed: 8071367]

Riessen R, Fenchel M, Chen H, Axel DI, Karsch KR, Lawler J. Cartilage oligomeric matrix protein (thrombospondin-5) is expressed by human vascular smooth muscle cells. Arterioscler Thromb Vasc Biol. 2001; 21:47–54. [PubMed: 11145932]

Risher WC, Eroglu C. Thrombospondins as key regulators of synaptogenesis in the central nervous system. Matrix Biol. 2012; 31:170–177. [PubMed: 22285841]

Roberts DD, Miller TW, Rogers NM, Yao M, Isenberg JS. The matricellular protein thrombospondin-1 globally regulates cardiovascular function and responses to stress via CD47. Matrix Biol. 2012; 31:162–169. [PubMed: 22266027]

Rosenberg RD, de Agostini AI. New approaches for defining sequence specific synthesis of heparan sulfate chains. Adv Exp Med Biol. 1992; 313:307–316. [PubMed: 1442267]

Rumsey SC, Obunike JC, Arad Y, Deckelbaum RJ, Goldberg IJ. Lipoprotein lipase-mediated uptake and degradation of low density lipoproteins by fibroblasts and macrophages. J Clin Invest. 1992; 90:1504–1512. [PubMed: 1401083]

Shimada K, Gill PJ, Silbert JE, Douglas WH, Fanburg BL. Involvement of cell surface heparin sulfate in the binding of lipoprotein lipase to cultured bovine endothelial cells. J Clin Invest. 1981; 68:995–1002. [PubMed: 6457061]

Smith JP, Hicks PS, Ortiz LR, Martinez MJ, Mandler RN. Quantitative measurement of muscle strength in the mouse. J Neurosci Methods. 1995; 62:15–19. [PubMed: 8750080]

Sodersten F, Ekman S, Schmitz M, Paulsson M, Zaucke F. Thrombospondin-4 and cartilage oligomeric matrix protein form heterooligomers in equine tendon. Connect Tissue Res. 2006; 47:85–91. [PubMed: 16754514]

Stenina OI, Byzova TV, Adams JC, McCarthy JJ, Topol EJ, Plow EF. Coronary artery disease and the thrombospondin single nucleotide polymorphisms. Int J Biochem Cell Biol. 2004; 36:1013–1030. [PubMed: 15094117]

Stenina OI, Desai SY, Krukovets I, Kight K, Janigro D, Topol EJ, Plow EF. Thrombospondin-4 and its variants: expression and differential effects on endothelial cells. Circulation. 2003; 108:1514–1519. [PubMed: 12952849]

Stenina OI, Topol EJ, Plow EF. Thrombospondins, their polymorphisms, and cardiovascular disease. Arterioscler Thromb Vasc Biol. 2007; 27:1886–1894. [PubMed: 17569883]

Svensson L, Aszodi A, Heinegard D, Hunziker EB, Reinholt FP, Fassler R, Oldberg A. Cartilage oligomeric matrix protein-deficient mice have normal skeletal development. Mol Cell Biol. 2002; 22:4366–4371. [PubMed: 12024046]

Sweetwyne MT, Murphy-Ullrich JE. Thrombospondin1 in tissue repair and fibrosis: TGF-beta-dependent and independent mechanisms. Matrix Biol. 2012; 31:178–186. [PubMed: 22266026]

Topol EJ, McCarthy J, Gabriel S, Moliterno DJ, Rogers WJ, Newby LK, Freedman M, Metivier J, Cannata R, O'Donnell CJ, Kottke-Marchant K, Murugesan G, Plow EF, Stenina O, Daley GQ. Single nucleotide polymorphisms in multiple novel thrombospondin genes may be associated with familial premature myocardial infarction. Circulation. 2001; 104:2641–2644. [PubMed: 11723011]

van Kuppevelt TH, Dennissen MA, van Venrooij WJ, Hoet RM, Veerkamp JH. Generation and application of type-specific anti-heparan sulfate antibodies using phage display technology. Further evidence for heparan sulfate heterogeneity in the kidney. J Biol Chem. 1998; 273:12960–12966. [PubMed: 9582329]

van Kuppevelt TH, Jenniskens GJ, Veerkamp JH, ten Dam GB, Dennissen MA. Phage display technology to obtain antiheparan sulfate antibodies. Methods Mol Biol. 2001; 171:519–534. [PubMed: 11450265]

Walton BWJ, Coresh J, Boerwinkle E. Thrombospondin-2 and Lymphotoxin-a gene variations predict coronary heart disease in a large prospective study. Circulation (Suppl). 2003; 108:IV–771.

Wessel J, Topol EJ, Ji M, Meyer J, McCarthy JJ. Replication of the association between the thrombospondin-4 A387P polymorphism and myocardial infarction. Am Heart J. 2004; 147:905–909. [PubMed: 15131549]

Williams KJ, Fless GM, Petrie KA, Snyder ML, Brocia RW, Swenson TL. Mechanisms by which lipoprotein lipase alters cellular metabolism of lipoprotein(a), low density lipoprotein, and nascent

lipoproteins. Roles for low density lipoprotein receptors and heparan sulfate proteoglycans. J Biol Chem. 1992; 267:13284–13292. [PubMed: 1320015]

Yamada Y, Izawa H, Ichihara S, Takatsu F, Ishihara H, Hirayama H, Sone T, Tanaka M, Yokota M. Prediction of the risk of myocardial infarction from polymorphisms in candidate genes. N Engl J Med. 2002; 347:1916–1923. [PubMed: 12477941]

Ye S, Luo Y, Lu W, Jones RB, Linhardt RJ, Capila I, Toida T, Kan M, Pelletier H, McKeehan WL. Structural basis for interaction of FGF-1, FGF-2, and FGF-7 with different heparan sulfate motifs. Biochemistry. 2001; 40:14429–14439. [PubMed: 11724555]

Zhang G, Ezura Y, Chervoneva I, Robinson PS, Beason DP, Carine ET, Soslowsky LJ, Iozzo RV, Birk DE. Decorin regulates assembly of collagen fibrils and acquisition of biomechanical properties during tendon development. J Cell Biochem. 2006; 98:1436–1449. [PubMed: 16518859]

Highlights

1. TSP-4 controls the deposition of ECM in tendon and skeletal muscle.
2. In tendon, TSP-4 deficiency results in altered structure of collagen fibrils.
3. TSP-4 deficiency results in impaired metabolism in red skeletal muscle.
4. TSP-4 deficiency causes incorrect modification of heparan sulfates and, as a result, decreased activity of lipoprotein lipase and loss of betaglycan (TGF® receptor III).
5. These changes result in decreased strength of the whole limb.

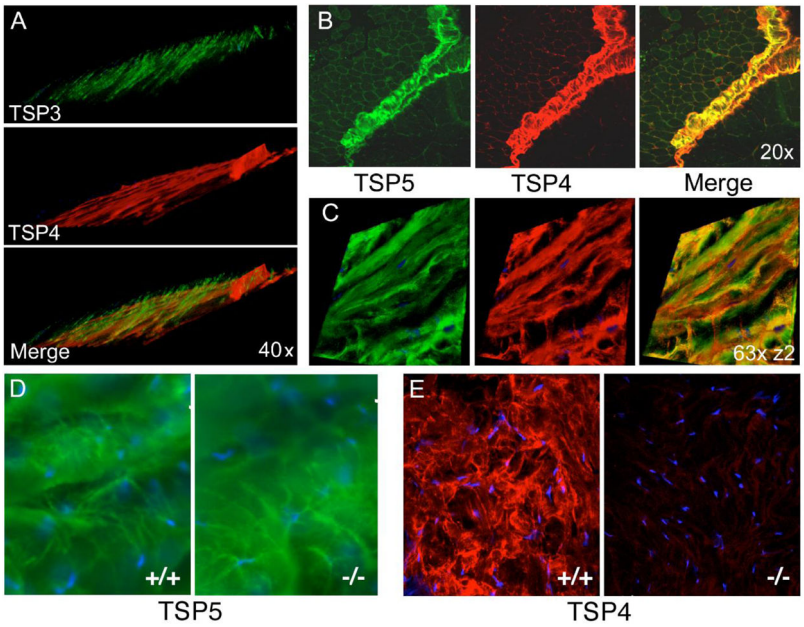

Figure 1. Expression of subgroup B thrombospondins in tendon

(A) 3-D reconstruction of TSP-4 and TSP-3 expression in WT triceps tendon showing different orientations of the two molecules as determined by immunohistochemistry. (B) Colocalization of TSP-4 and TSP-5 in perimysium and (C) in patellar tendon; immunohistochemical 3-D reconstruction. (D) Expression of TSP-5 does not change in *Thbs4*$^{-/-}$ tendon compared to WT. (E) Lack of TSP4 expression in *Thbs4*$^{-/-}$ patellar tendon. Nuclei (blue) were visualized by DAPI staining.

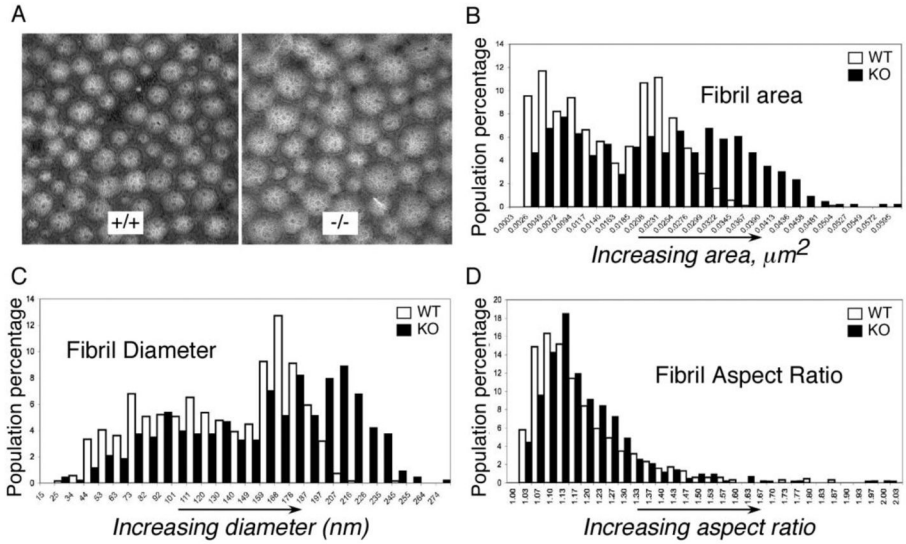

Figure 2. Collagen fibrils in tendon of *Thbs4*$^{-/-}$ mice

(A) Transmission electron micrographs (TEMS) of collagen fibrils in patellar tendon of *Thbs4*$^{-/-}$ (right) and WT (left) mice. Scale bars = 0.5 μm. Histograms of collagen fibril area (B), fibril diameter (C) and fibril aspect ratio (D) in WT mice (open bars, n = 5) and *Thbs4*$^{-/-}$ mice (black bars, n =5). Fibril areas and fibril diameters are more variable, and larger fibrils are more prevalent in patellar tendon of *Thbs4*$^{-/-}$ mice but the shapes of fibrils, assessed from the aspect ratio, are not altered.

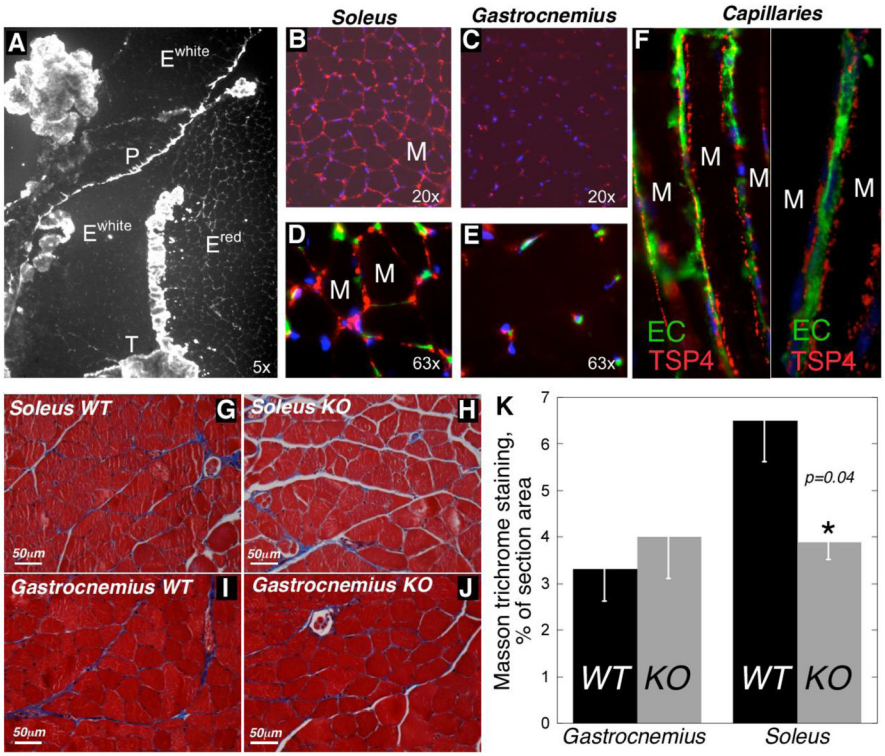

Figure 3. Expression of TSP4 in the skeletal muscle

(A) Expression of TSP-4 (white color) in triceps. TSP-4 is abundant in tendon (T), perimysium (P) and endomysium of soleus (E^{red}, also shown in B, D), whereas its amount is lower in the endomysium of gastrocnemius and plantaris (E^{white}, also shown in C, E). TSP-4 (red color) is seen close to endothelial cells, which are visualized by FITC-conjugated lectin staining (green) (D, E). M = myocyte in B and D. (F) Capillaries between soleus muscle fibers are surrounded by globular aggregates of TSP-4. M = myocyte. Nuclei (blue) are detected with DAPI (B – F). (G–J) ECM staining with Masson trichrome (ECM = blue color) in soleus (G, H) and gastrocnemius (I, J) of WT (G, I) and *Thbs4*$^{-/-}$ mice (H, J). (K) Quantification of ECM in the skeletal muscles of WT and *Thbs4*$^{-/-}$ mice (% of area stained with Masson trichrome).

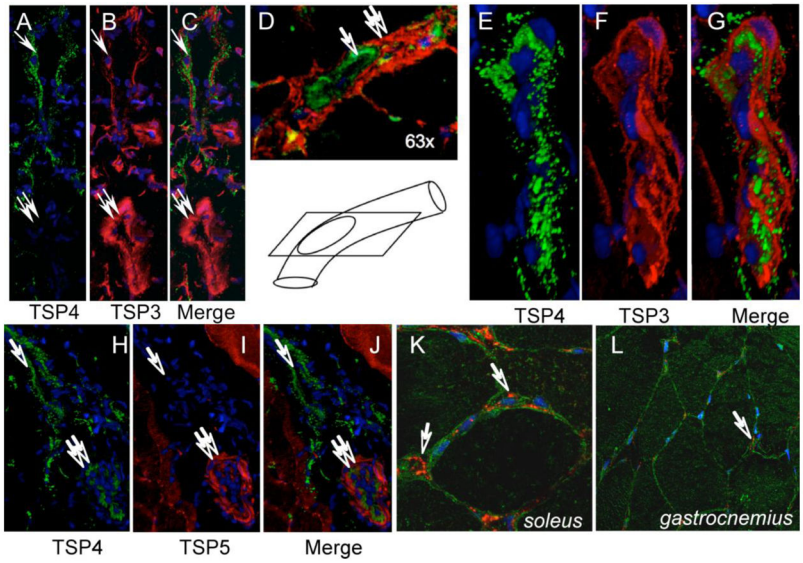

Figure 4. Non-overlapping localization of TSP-3, TSP-5 and TSP-4 in blood vessels

(A) Expression of TSP-3 (red) and TSP-4 (green) in vascular wall: TSP-3 is present in both vein (single arrow) and artery (double arrow). TSP-4 was not detected in all the arteries, while TSP-3 was always found in tunica media of arteries (double arrow). (D) Non-overlapping expression of TSP-3 (green, single arrow) and TSP-4 (red, double arrow) in the vascular wall. The vessel was sectioned in the direction shown in the cartoon, lower panel. (E–G) In the wall of veins, both TSP-4 and TSP-3 are detected in non-overlapping staining pattern. (H–J) TSP-4 (green) is consistently expressed in the vein wall, while no TSP-5 (red) expression is detected in veins (single arrow). In arteries, TSP-5 is expressed in tunica media. (K,L) TSP-5 (green) is expressed around muscle fibers, whereas TSP-4 (red) is found close to capillaries (arrow).

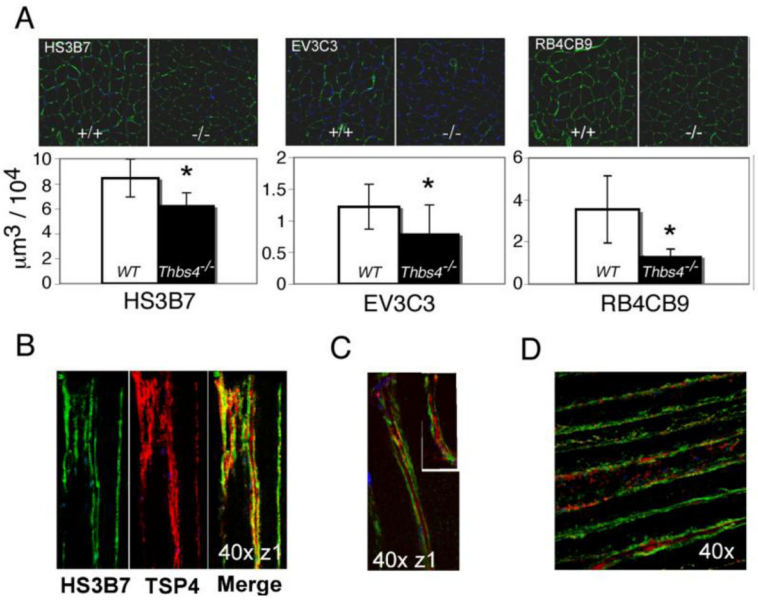

Figure 5. Differential expression of specific heparan sulfate epitopes in soleus of *Thbs4*$^{-/-}$ mice

(A) Expression of HS epitopes (green) recognized by HS3B7, EV3C3, and RB4CB9 antibodies in soleus. Upper panels – immunohistochemistry, representative images. Lower panels: Reduced amount of the epitopes was recognized by HS3B7, EV3C3, and RB4CB9 antibodies in soleus of *Thbs4*$^{-/-}$ mice (shaded bars) compared to WT mice (open bars). (B–D) HS are localized on the surface or in basal lamina of myofibers. TSP-4 (red) colocalizes with the (B) HS3B7 (green) epitope and locates between the GAGs in close proximity to (C) EV3C3 (green) and (D) RB4CB9 (green) epitopes.

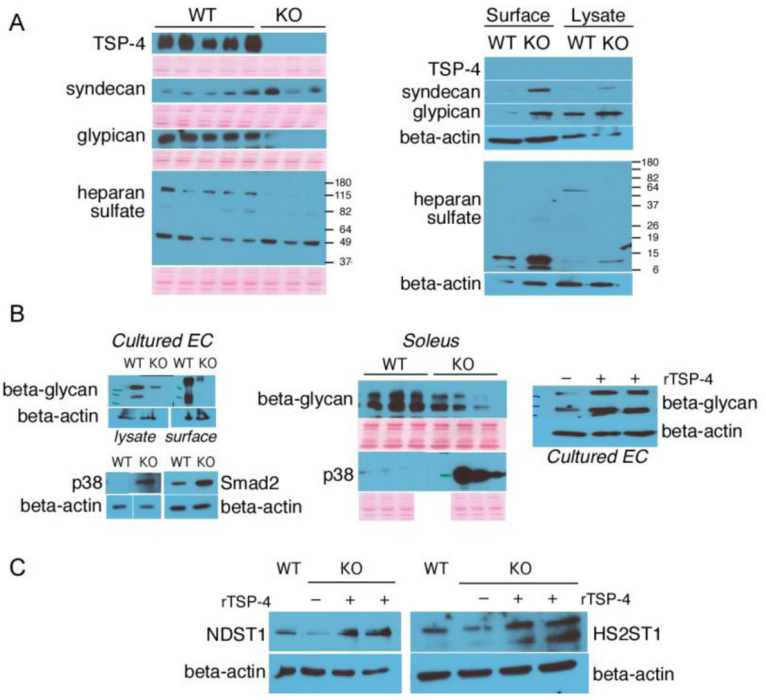

Figure 6. Levels of Heparan Sulfate core proteins

(A, left panel) soleus protein extracts; (A, right panel) cultured mouse EC; (B) levels of beta-glycan and activation of intracellular signaling mediators in cultured EC and muscle tissue extracts; (C) levels of key enzymes controlling the synthesis and modifications of HS in cultured EC by Western blotting.

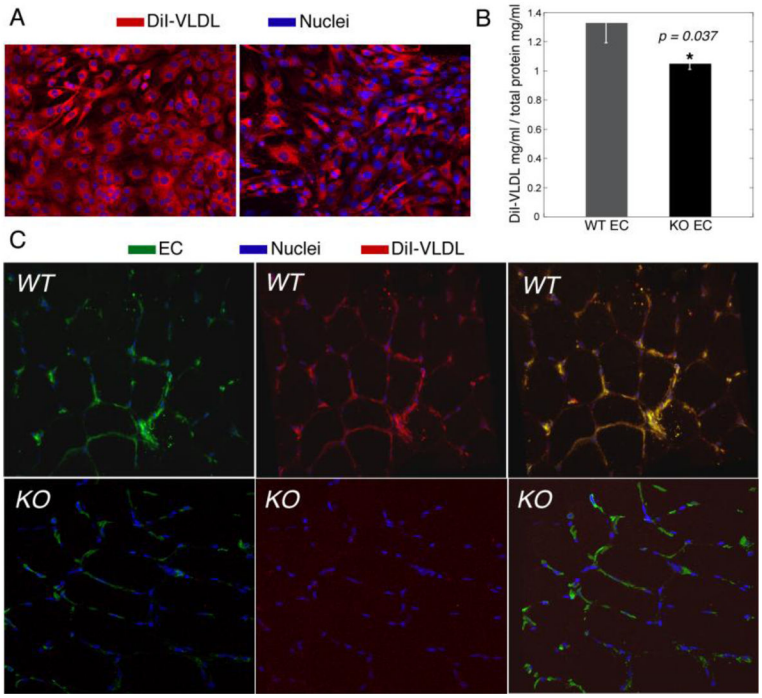

Figure 7. Uptake of VLDL by EC of *Thbs4*$^{-/-}$ and WT mice

(A, B) Uptake of DiI-VLDL by cultured EC: (A) representative image by immunofluorescence, confocal microscopy; (B) quantification of fluorescence. (C) Uptake of DiI-VLDL by EC in soleus of *Thbs4*$^{-/-}$ (KO) and WT (WT) mice.

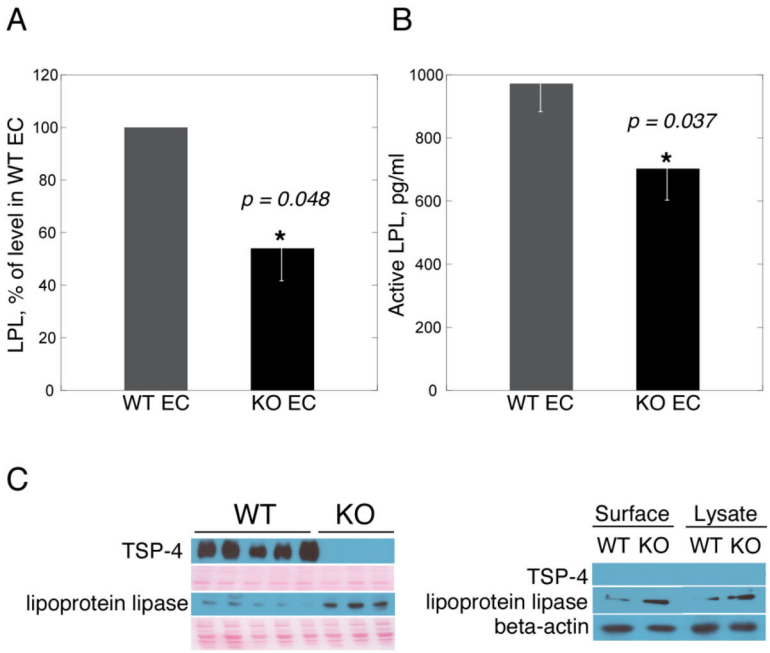

Figure 8. Activity and expression of endothelial LPL in *Thbs4*$^{-/-}$ mice

(A) activity in cultured EC; (B) activity of LPL *in vivo* in plasma of *Thbs4*$^{-/-}$ and WT mice calculated as a difference between the activity before and after heparin injection; (C) Levels of LPL in cultured mouse EC: left panel – soleus extracts from *Thbs4*$^{-/-}$ (KO) and WT (WT) mice with loading control (membrane stained with Ponceau S to visualize total protein); right panel – lysates of cultured EC from *Thbs4*$^{-/-}$ (KO) and WT (WT) mice with loading control (beta-actin).

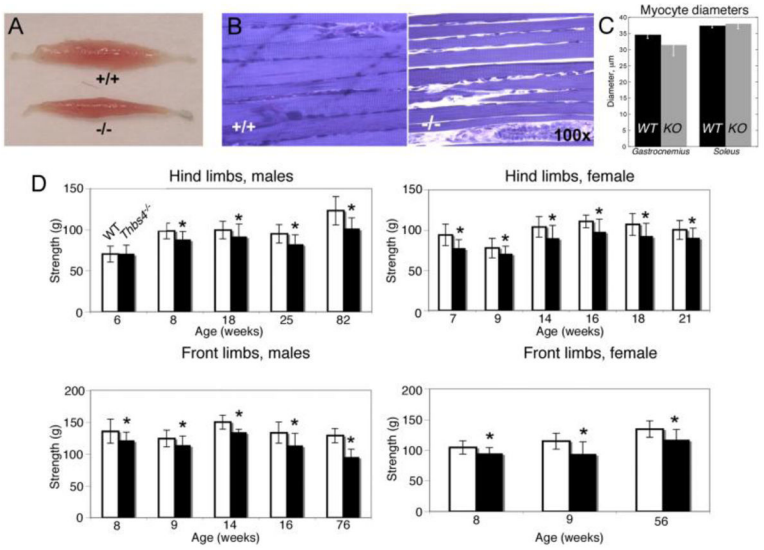

Figure 9. Muscle morphology and function are changed in *Thbs4*$^{-/-}$ mice

(A) Lower soleus muscle mass in WT and *Thbs4*$^{-/-}$ mice. (B) Muscle fibers of WT and *Thbs4*$^{-/-}$ soleus (note additional space between fibers that appeared during sample preparation). (C) Myocyte diameter in soleus and gastrocnemius of WT and *Thbs4*$^{-/-}$ mice. (D) Muscle strength of hind limbs (top panels) and front limbs (bottom panels) of males (left panels) and females (right panels) are decreased in *Thbs4*$^{-/-}$ as compared to WT mice (mean value ± standard deviations, *$p<0.05$, $3\leq n\leq 13$ for each age group, 6–8 trials were performed with each mouse in recording limb strength).

Matrix Biol. Author manuscript; available in PMC 2015 July 01.

Table 1

Metabolic changes in *Thbs4*$^{-/-}$ mice

Glucose, insulin, non-esterified fatty acids (NEFA), total cholesterol, VLDL, LDL (not shown – no difference), and HDL (not shown – no difference) were measured in WT and *Thbs4*$^{-/-}$ mice at age 8 weeks, 20 weeks, and 35 weeks. Blood from mice on normal chow diet and from mice on high carbohydrate diet (started at 4 weeks of age) was used. In mice on chow diet, NEFA were measured in fasted mice and in mice that received oil gavage. NEFA were also measured at 55 weeks of age and were found significantly different between WT and *Thbs4*$^{-/-}$ mice. Only statistically significant changes ($p < 0.05$)are shown in the table. Data from fasted mice on chow diet without further manipulation are not shaded, data from mice on high carbohydrate content diet and mice after the oil gavage are shaded.

	Glc, mg/dL	**Glc, mg/dL, *high carb***	**Insulin, ug/L**	**Insulin, Ug/L, *high carb***	**NEFA**	**NEFA, mmol/L *oil gavage***	**Cholester, mg/dL *high carb***	**VLDL, mg/dL, *high carb***
8 weeks	8 weeks	8 weeks	8 weeks	8 weeks	8 weeks	8 weeks	8 weeks	8 weeks
KO, n=5	74.8±14					0.44±0.08		
WT, n=4	96.5±18					0.61 ±0.03		
p	0.018					0.006		
20 weeks	20 weeks	20 weeks	20 weeks	20 weeks	20 weeks	20 weeks	20 weeks	20 weeks
KO, n=11			0.19±0.09					
WT, n=12			0.36 ±0.23					
p			0.028					
35 weeks	35 weeks	35 weeks	35 weeks	35 weeks	35 weeks	35 weeks	35 weeks	35 weeks
KO, n=5–10	106±9.9	152±23		1.68±0.41			144±35	14±3.6
WT, n=5–12	124±12.8	177±27.5		3.01±1.02			100±9.5	9.3±3.25
p	0.014	0.021		0.0012			0.049	0.04
55 weeks	55 weeks	55 weeks	55 weeks	55 weeks	55 weeks	55 weeks	55 weeks	55 weeks
KO, n=6					0.67±0.09			
WT, n=10					0.85 ±0.1			
p					0.015			